ACTA IMEKO
ISSN: 2221-870X
June 2025, Volume 14, Number 2, 1 - 9

Uncertainty analysis in the estimation of construction and demolition wastes emissivity through infrared thermography

Giovanni Salerno[1], Gloria Cosoli[2], Maria Teresa Calcagni[1], Giuseppe Pandarese[1], Gian Marco Revel [1]

[1] *Dipartimento di Ingegneria Industriale e Scienze Matematiche, Università Politecnica delle Marche, Via Brecce Bianche 12, 60131 Ancona, Italy*
[2] *Dipartimento di Scienze Teoriche ed Applicate, Università eCampus, Via Isimbardi 10, 22060 Novedrate, Italy*

ABSTRACT
Construction and demolition wastes (CDWs) represent one of the largest slices of global waste and can be a significant source of reusable materials in the context of sustainable and circular construction practices. The accurate characterization of these materials can be critical to improve recycling and valorisation processes. In this study, a measurement procedure is proposed for the characterization of CDWs using active infrared thermography to estimate the emissivity of the materials commonly used in this context. The material classes analysed are concrete, bricks, tiles and ceramic, wood, plastic, metals, paper and cardboard, and mixed CDWs. An experimental test protocol is defined for heating specimens and acquiring thermal images, allowing the accurate estimation of their emissivity based on a paint and a tape with known emissivity used as reference. To ensure the reliability and robustness of the estimated emissivity values, an uncertainty analysis is performed using a Monte Carlo simulation evaluating the impact of the uncertainty ($u(x_i)$) related to the known emissivity value of the reference paint (0.89 ± 0.01, reported as mean ± standard deviation) on the results. The results show that the input uncertainty propagates along the measurement chain, leading to an output uncertainty ($u_i(y)$) at least doubled for all classes, and more than doubled for the plastic class.

Section: RESEARCH PAPER

Keywords: CDWs; material characterization; active infrared thermography; measurement uncertainty analysis

Citation: G. Salerno, G. Cosoli, M. T. Calcagni, G. Pandarese, G. M. Revel , Uncertainty analysis in the estimation of construction and demolition wastes emissivity through infrared thermography, Acta IMEKO, vol. 14 (2025) no. 2, pp. 1-9. DOI: 10.21014/actaimeko.v14i2.2056

Section Editor: Andrea Scorza, University Roma Tre, Italy

Received January 21, 2025; **In final form** May 28, 2025; **Published** June 2025

Funding: This research activity was carried out within the RECONSTRUCT (A Territorial Construction System for a Circular Low-Carbon Built Environment) project, funded by the European Union's Horizon Europe research and innovation programme under grant agreement no. 101082265.

Corresponding author: Gloria Cosoli, e-mail: gloria.cosoli@uniecampus.it

1. INTRODUCTION

The construction sector is one of the most impactful on the waste generation count, specifically construction and demolition wastes (CDWs) represent approximately one third of the total amount of waste generated in Europe [1]. Among the most used materials it is possible to mention concrete, wood, plastic, metals, etc., and reusing most of them could be very beneficial from both economic and sustainability perspectives. Digital technologies can play a fundamental role to improve the processes of CDWs sorting [2], exploiting vision and artificial intelligence (AI) techniques to achieve a detailed characterization of those materials, with the ultimate aim of their valorisation in the perspective of a more sustainable and circular construction sector.

Many studies, focusing on the recognition of CDWs materials, rely on machine learning (ML), AI, and robotics [3], [4]. However, these techniques commonly use only visible images and thus the ability to characterize materials is limited. Usually, they are exploited in laboratory, under controlled conditions. Furthermore, artificial neural networks require large amounts of data/images, and time to label them and train models to distinguish one material from another. Sensing and digital technologies can make a relevant contribution in this context and equipment of different types can be exploited.

In literature, many studies have used a wide variety of sensors and measurement solutions. For example, near-infrared (NIR) sensors were used to assess the quality of mixed recycled aggregates and improve sorting separating the different types of materials on a conveyor belt [5]. Serranti et al. [6] used

hyperspectral cameras to recognize various materials and substances in CDWs, especially the presence of hazardous materials such as asbestos. In [7] the possibility to recognize and classify different types of recycled aggregates with respect to different contaminants (e.g., brick, gypsum, plastic, etc.) using the hyperspectral camera located on a conveyor belt was explored. Considering the wide adoption of industrial cameras, some studies have considered the possibility of developing artificial intelligence-based software to perform the selection of various materials [8] or segment the different classes of CDWs [9]. The combination of several different types of sensors has also been evaluated; for example, in [10] a visible camera, a short-wave infrared sensor (SWIR), and a multi spectral sensor were employed on a conveyor belt for the recognition, and a robotic arm was used to sort the different material. In [11] the authors proposed different solutions using visible camera, LiDAR or depth sensor, and infrared (IR) thermal camera to recognize the type and quantity of different CDWs materials. The hyperspectral camera and the X-ray fluorescence (XRF) were used in [12] for the characterization of post-earthquake CDWs; visible camera and thermal information were used in [13] to differentiate the CDW. Radica et al. [14] made us of micro-XRF and NIR spectroscopy to assess the chemical composition of CDW specimens in order to optimize the recycling process. For the NIR spectroscopy, a SWIR camera was used in the range 1000-2500 nm, dividing the analysis in three main regions (i.e., 1330–1680, 1830–2140, and 2140–2400 nm) to identify certain molecules and/or materials present. In [15] a material characterization was carried out using Fourier transform infrared (FTIR) spectroscopy as reference method, and hyperspectral analysis using a portable NIR spectrometer and a hyperspectral camera operating in the spectral ranges of, respectively, 1000-1650, 450-900 nm. The aim was to evaluate the spectral footprint of CDWs materials and to provide useful information in a view of CDWs valorisation.

Considering the wide field of application of thermal imaging cameras at an industrial level and given the differences in emissivity between different material categories, some studies decided to base the classification of different types of materials on IR thermography. Gundupalli et al. [16] developed a method to detect metallic (aluminium and copper) and non-metallic materials (plastic, printed circuit boards, and glass) using active thermography to analyse the waste passing on a conveyor belt. A study [17] presents a similar method (active thermography on conveyor belt) applied to municipal waste to characterize different material classes (iron, wood, plastic, paper, etc.) achieving very good results (with a classification accuracy ranging from 85 % to 96 %). Bai et al. [18] used an alternative method with respect to the traditional active thermography, heating up the specimens for a brief time with a lamp for the acquisition of thermal images. These images were then analysed by ML algorithms to detect different types of materials (concrete, cardboard, wood, aluminium, etc.). They obtained accurate results for some types of materials (rubber: accuracy up to 94.5 %, wood: accuracy up to 93.1 %), worse for other types (steel: accuracy up to 58.4 %, and aluminium: accuracy up to 65.6 %). Some studies were focused on the estimation of material emissivity; in [19] the authors carried out infrared thermography tests to estimate the emissivity of several types of rocks, basing the evaluation on a known emissivity tape as a reference. Harrap et al. [20] employed the combination of thermal camera and thermocouples to estimate the emissivity of different parts of flowers. A similar technique was used in [21] to estimate the emissivity of calcium-magnesium-alumina-silicates materials, with the difference that the working temperature was very high (T>800 °C).

Despite advancements in digital technologies, existing methods for classifying CDWs still have several limitations. Many approaches rely solely on visible images, limiting their ability to differentiate materials with similar appearance but different physical properties. On another hand, ML and AI-based methods require large, labelled datasets and controlled operating conditions, making them difficult to be implemented in real-world scenarios [3], [4]. Hyperspectral imaging (HSI) and X-ray fluorescence, while effective, require expensive and complex equipment that is not always feasible for large-scale waste sorting [6], [7], [12].

Although thermography has been used for materials classification, most studies have focused on temperature differences rather than estimating emissivity, a critical parameter both for ensuring reliable temperature measurement and for improving classification accuracy [16]-[19].

This study evaluates the potential of thermal analysis using an infrared camera. The materials of interest are those widely used in the construction field and most likely to be found in CDWs. The aim is to estimate the emissivity value of these materials, performing infrared tests in controlled laboratory conditions on a certain number of specimens, so as to consider the intrinsic variability of these materials. The emissivity values are estimated based on the comparison with a paint or tape of known emissivity used as reference. This study can be considered as preliminary for the development of such a measurement approach, due to the limitation of the quantity of data used; in fact, to provide information within a certain confidence interval, an uncertainty analysis was carried out using the Monte Carlo method. The uncertainty analysis evaluated how the input uncertainty ($u(x_i)$), i.e., the uncertainty related to the known emissivity value of the reference paint as provided by the manufacturer, propagates through the entire measurement chain resulting in a certain output uncertainty ($u_i(y)$). The uncertainty analysis was performed for each material class analysed using paint with known emissivity.

This research activity was carried out within the RECONSTRUCT (A Territorial Construction System for a Circular Low-Carbon Built Environment) project, funded by the European Union's Horizon Europe research and innovation programme under grant agreement no. 101082265.

2. MATERIALS AND METHODS

This section describes the types of materials characterised, the equipment employed for testing, the experimental test procedure, and the data processing pipeline.

2.1. CDW classes

The CDWs materials considered for characterization are among the most essential and widely used in the construction sector; in Table 1 these materials are listed along with their respective European Waste Codes (EWC) [22].

The specimens were provided by the project partners COMSA (Barcelona, [23]) and Sorigué (Barcelona, [24]), collected from their sites (in Figure 1 an example of specimen for each class). The source sites are construction and waste management sites, respectively.

The specimens were distributed among the different classes to ensure a representative number of specimens in each category

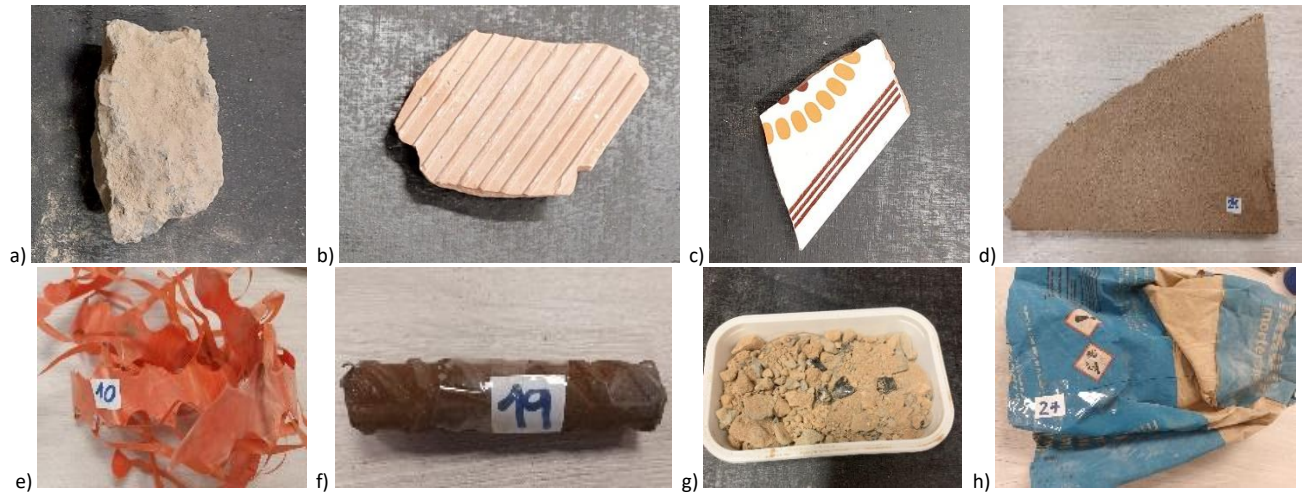

Figure 1. Examples of specimens per class: a) concrete, b) bricks, c) tiles and ceramic, d) wood, e) plastic, f) metals, g) mixed CDWs, h) paper and cardboard.

in order to have a significant dataset, properly including the intrinsic variability of these materials.

2.2. Emissivity estimation using active thermography

The primary objective of this study is to estimate the relative emissivity of CDWs material classes using active thermography, particularly the hemispherical spectral emissivity.

The thermal camera is able to measure the radiance emitted by a body/object; if the emissivity of the object is known, the temperature can be computed based on the Stefan-Boltzmann law (1):

$$E = \sigma T^4 , \tag{1}$$

where:

- E in $\mathrm{W\,m^{-2}}$ represents the total radiant exitance (heat flux) emitted from the surface,
- $\sigma = 5.67 \cdot 10^{-8}\ \mathrm{W\,m^{-2}\,K^{-4}}$ is the Stefan-Boltzmann constant
- T in K is the absolute temperature of the surface.

Since the thermal camera detects only emission within its spectral range, the Planck's law (strongly related to Stefan-Boltzmann law), which defines spectral radiance exitance by wavelength, was applied. If the sensor is wideband and the measured spectral distribution is assumed to be representative of the total emitted radiation, Stefan-Boltzmann law can be considered valid.

This law is valid for black bodies, which are ideal surfaces that absorb all the radiant incident energy; for a real object it is necessary to add a correction multiplicative factor, i.e., ε_r, the relative emissivity of the surface, that is formulated as the ratio between the radiation emitted by the surface and the radiation emitted by a black body in the same conditions (in terms of temperature, directions, and spectral band considered). Thus, the Stefan-Boltzmann law can be rewritten in (2):

$$E = \sigma \varepsilon_r T^4 . \tag{2}$$

The aim is to measure the actual temperature of a specimen of known emissivity value (i.e., reference material) and estimate the emissivity of another specimen (i.e., test material, to be characterized), assuming the thermal equilibrium between the two.

If the emissivity set in the camera software is the reference emissivity, the reference temperature is correctly determined; the actual test temperature is the same as the reference temperature, but the measured test temperature is different due to the mismatch in emissivity [25]. Based on this observation, it is possible to write the Equation (3):

$$E_{\mathrm{test}} = \sigma \varepsilon_{\mathrm{r,test}} T_{\mathrm{test}}^4 = \sigma \varepsilon_{\mathrm{r,ref}} T_{\mathrm{test,meas}}^4 , \tag{3}$$

where:

- E_{test} in $\mathrm{W\,m^{-2}}$ is the radiant exitance of the specimens, measured by the thermal camera,
- $\varepsilon_{\mathrm{r,test}}$ is the test material emissivity (unknown),
- $\varepsilon_{\mathrm{r,ref}}$ is the material reference emissivity,
- T_{test} in K is the actual test temperature, which is equal to reference temperature,
- $T_{\mathrm{test,meas}}$ in K is the measured test temperature.

Considering the thermal equilibrium between test and reference specimens, the Equation (3) can be rewritten as (4):

$$\varepsilon_{\mathrm{r,test}} = \left(\frac{T_{\mathrm{test,meas}}}{T_{\mathrm{ref}}}\right)^4 \varepsilon_{\mathrm{r,ref}} . \tag{4}$$

Throughout the text, for the sake of brevity, the term "emissivity" will be used to refer to relative emissivity.

2.3. Equipment and experimental procedure

The thermal camera used in this study is the VarioCam 980HD (Infratec, Dresden, Germany [26]), equipped with a microbolometer Focal Plane Array (FPA) IR sensor, and operating in a spectral band between 7.5 and 14.0 μm, with a measurement accuracy of ± 1.5 °C or ± 1.5 %. Data acquisition was performed using the software Irbis 3 plus (Infratec,

Table 1. Lists of materials and related EWC codes.

Material	EWC code
Concrete	17.01.01
Bricks	17.01.02
Tiles and ceramic	17.01.03
Wood	17.02.01
Plastic	17.02.03
Metals	17.04
Mixed CDWs	17.09.04
Paper and cardboard	15.01.01

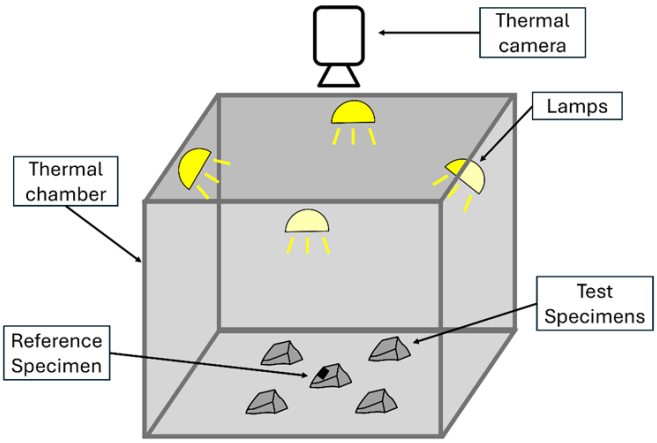

Figure 2. Experimental setup for tests with IR thermography.

Dresden, Germany, v. 3.0.0 [26]), used for the focus of the camera, the acquisitions, and to save and export the data.

Table 2 summarizes the numbers of tested specimens per class, and the main details of the tests.

A group analysis was possible when the specimens were of the same material and very similar in terms of dimension and shape; for the concrete, brick, and tile and ceramic classes, a group analysis was performed for 5 out of 6 specimens, while the remaining one was analysed individually.

For the tiles and ceramic class, the two sides were tested and analysed separately, and in the Section 3 they are presented as separate classes (as they are significantly different); on the other hand, for the paper and cardboard class, two sides/parts of each specimen were analysed but in the results they were considered as one class.

The specimens were prepared for the tests applying a paint or a tape with known emissivity. The paint used was the Aremco HiE-Coat-840-C (Valley Cottage, NY, United States [27]), which has an emissivity of ε_r = 0.89 with a measurement uncertainty of 0.01 (reported in terms of standard deviation); this value was obtained as a weighted average of the emissivity values in the considered spectral band, i.e., 7.5-14.0 μm, and considering the operative temperature range (in the order of ambient temperature). On the other hand, the tape is a standard known emissivity tape with an emissivity value of ε_r = 0.93.

For the application of the paint, it was necessary to cure the specimen in an oven at 100 °C for an hour for the proper adhesion of the paint (according to the manufacturer's recommendations), and this was not possible for all the specimens. The paint was preferrable to the tape; however, in certain cases/for some materials it was not possible to apply the paint due to the type of surfaces (such as for some samples of plastic or the glazed side of tiles), hence the tape was used.

Figure 3. Example of mixed CDWs specimen.

Table 2. Summary of specimen characteristics and testing approach.

Material	Number of specimen	Reference type	Acquisition type	Sides analysed
Concrete	6	Paint	Group or individual	One
Bricks	6	Paint	Group or individual	One
Tiles and ceramic	6	Paint or tape	Group or individual	Both
Wood	3	Paint or tape	Individual	Both
Plastic	15	Paint or tape	Individual	One
Metals	5	Paint or tape	Individual	One
Mixed CDWs	2	Tape	Individual	One
Paper and cardboard	4	Paint	Individual	One or both

The experimental setup is illustrated in Figure 2. The pipeline related to the experimental procedure is reported hereafter:

- The specimen (or group of specimens) was positioned in the thermal chamber, where it can be isolated from external sources of interference during measurements, and where there are four halogen lamps (1100 W in total) to heat up the specimens (Figure 2). The chamber, made of aluminium, measured (95 × 80 × 40) cm³ (length × width × height).
- The thermal camera was focused using the dedicated software.
- The lamps were switched on and the specimens were heated up until + 8-12 °C above the ambient temperature (20-25 °C); the temperature increment was monitored through the software by observing the temperature of the reference area. The range of increase (8-12 °C) is wide because at + 8 °C the halogen lamps were switched off, but they continued to heat in an uncontrolled mode because they were hot; for some samples this led to a further increase up to + 12 °C.
- The acquisition of a 60-s sequence was started, with an acquisition rate of one frame per second (fps) – i.e., a sampling frequency equal to 1 Hz.
- The lamps were switched off just after the start of the acquisition.

For the class of mixed CDWs (Figure 3), a different approach was adopted: paint was applied to one of the specimen pieces, and as each sample was a mix of materials inside a container, and since the data analysis performed was different (Section 2.4), they were shuffled after each test to (presumably) include all the parts present in the mixed CDWs specimen in the acquisition (making sure to leave the area with the paint at known emissivity visible).

2.4. Data processing

The acquired data were exported as .csv files using the software Irbis 3 plus (as for the acquisition) and analysed using Python programming language to compute the emissivity value

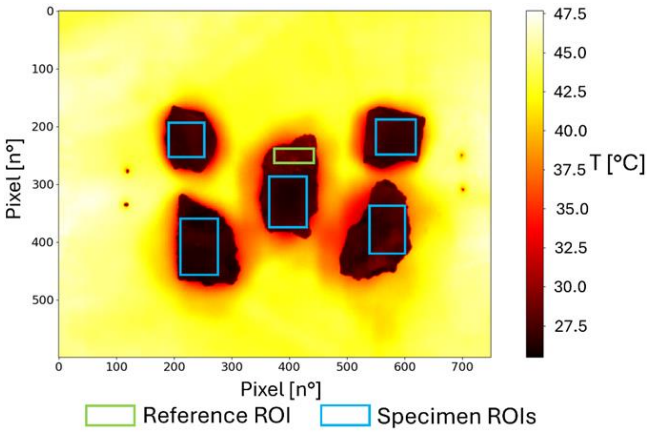

Figure 6. Example of thermal image with reference (green) and test (blue) ROIs.

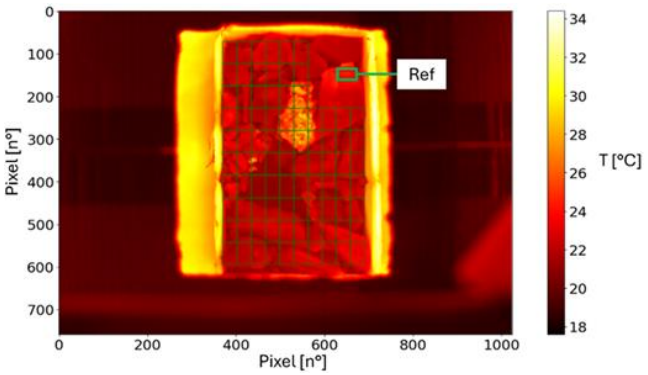

Figure 4. Example of thermal image of mixed CDWs.

for each region of interest (ROI) considered. The software allows to export a .csv file for each frame of the acquired sequence. The .csv files contain the measured temperature data for each pixel. An example of thermal image and analysed ROIs for reference and test materials is reported in Figure 6, where the reference ROI is the area with the reference paint.

The ROIs were selected interactively using a graphical user interface made for this use case in Python programming language to facilitate the selection of different ROIs for each test. It is worthy to note that not all the identified ROIs had the same number of pixels; this is due to the fact that the analysed specimens had different geometries and dimensions.

Although the acquired sequences consist of 60 frames, only 10 of these were used for analysis, and these are those during the cooling phase just after the lamps were switched off. The acquisition was still done by 60 frames to be sure to include the cooling duration.

The computation of the material emissivity was based on the comparison between the specimen(s) (i.e., test material) and the reference area in the thermal frame, and on the thermal equilibrium. The thermal equilibrium was assumed due to similar shape and size, same material, and by positioning them in a thermally controlled environment, which is isolated from external sources of interference. Hence, the emissivity was computed according to the Equation (4), considering as reference and test temperatures the average temperature of the respective ROIs.

The approach for the mixed CDWs class was based on one piece of material that is a reference (i.e., covered with paint) and the definition of many small ROIs, subsequently compared to the reference ROI (Figure 4). Each small ROI was considered as a specimen, and the results were obtained by averaging the emissivity value obtained for each ROI from the three tests done on the two containers.

Each specimen was analysed three times, repeating the test in the same operating conditions; the average value of emissivity for each specimen was computed, and, finally, the results from the specimens of the same class (material) were grouped together. Hence, the average and the standard deviation of their emissivity values were calculated to derive the emissivity of that material, expressed in terms of mean and standard deviation.

In Figure 5 illustrates the overall workflow, outlining the main steps from physical testing to data acquisition and processing.

2.5. Uncertainty analysis

The measurement uncertainty must be examined to provide a classification within a certain confidence interval.

The estimation of the measurement uncertainty was performed for each material class considered by employing three different datasets:

- A single test on a single specimen.
- 3 repeated tests on a same specimen, to include intra-specimen variability.
- 3 repeated tests on 5 different specimens (or different portions), to include also inter-specimen variability.

It is important to highlight that the datasets are incremental, with each dataset including also the data of the previous one.

To express the measurement uncertainty, the Monte Carlo method was adopted; at least 10^6 iterations were performed for each of the three tests to be able to express the 95 % confidence interval (using a coverage factor $k = 2$) according to the Guide to Expression of Measurement Uncertainty (GUM) [28].

The uncertainty analysis was focused on the tests performed considering the high-emissivity paint as reference, given that the manufacturer provides detailed technical specification on the uncertainty affecting the emissivity of the paint (contrarily to the tape, whose emissivity is reported without the related confidence interval). Hence, in the uncertainty analysis the input uncertainty was the one related to the reference paint emissivity ε_r, expressed as the standard deviation value provided by the manufacturer, in the spectral range analysed by the thermal camera, i.e., $\sigma = 0.01$. Consequently, the related expanded uncertainty (coverage factor $k = 2$) was equal to 0.02 (95 %

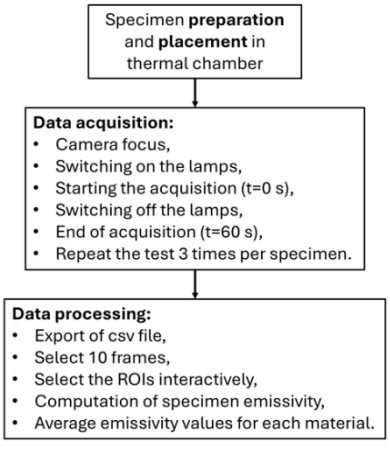

Figure 5. Block diagram summarizing the overall process, from testing to data acquisition and processing.

confidence interval). It is worthy to note that there can be other non-controllable operating conditions and experimental factors (e.g., the setting parameters of the ROIs, measurement uncertainty of the equipment, etc.) that could affect the results; the related variability was considered as part of the input variability reported above.

This additional analysis was performed only on the CDWs classes with at least 5 specimens tested with the paint, or 5 different portions of one (or more) specimens analysed (as for the paper class).

Uncertainty was evaluated by applying a perturbation (p) to the reference emissivity value and substituting the new emissivity value ($\varepsilon_{r,new} = 0.89 \pm p$) for the one previously set ($\varepsilon_r = 0.89$) to calculate the emissivity of the tested specimens. These perturbations were generated using a Gaussian distribution with a standard deviation equal to the value specified by the paint manufacturer ($\sigma = 0.01$). Finally, the resulting distribution of the 10^6 iterations were considered to calculate the mean and standard deviation of the emissivity obtained for each of the three tests and for each material class. The standard deviations obtained are taken into account to understand how much the input uncertainty related to the known emissivity value of the reference paint, affects the variability of the final emissivity values obtained for the CDW classes analysed.

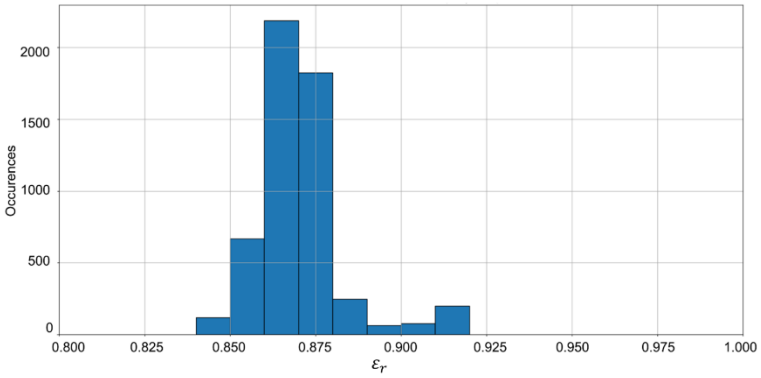

Figure 7. Mixed CDWs analysis: emissivity values distribution.

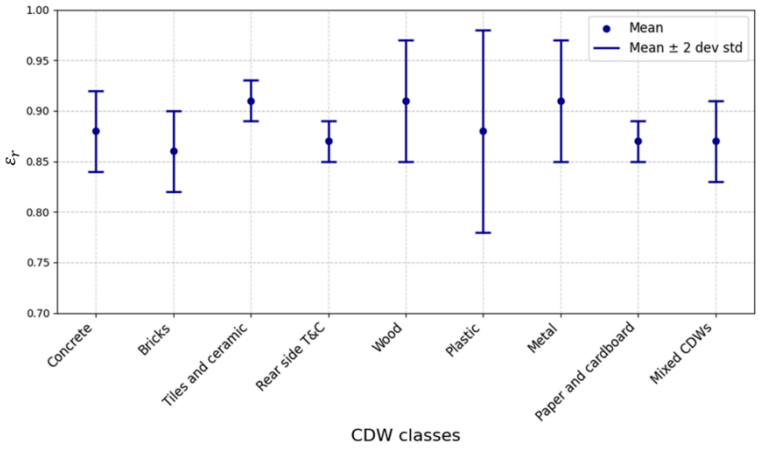

Figure 8. Emissivity 95 % confidence intervals (obtained from mean and standard deviation values, selecting a coverage factor $k = 2$).

3. RESULTS

3.1. Results on emissivity estimation

Table 3 presents the results of the emissivity estimation for each CDWs class, reported as minimum, maximum, mean, and standard deviation values. The number of measurements is the total number of frames analysed for each class; it is obtained by multiplying the number of specimens by the number of tests by 10 (number of frames considered in the analysis per test). For the tiles and ceramic class two sides were analysed for each sample, but the results were split since the two sides are totally different. For the wood class, each specimen was analysed in two different portions, but the results were grouped together since the material inspected is the same. The same was done for 2 out of 4 specimens of paper and cardboard class.

Table 3. Material emissivity: mean (Mean), minimum (Min), maximum (Max), and standard deviation (σ) values.

CDWs class	ε_r				number of measurements
	Mean	Min	Max	σ	
Concrete	0.88	0.84	0.91	0.02	180
Brick	0.86	0.81	0.91	0.02	180
Tiles and ceramic	0.91	0.89	0.92	0.01	180
*Rear side of tiles	0.87	0.86	0.88	0.01	180
Wood	0.91	0.86	0.94	0.03	180
Plastic	0.88	0.67	0.96	0.05	450
Metals	0.91	0.84	0.94	0.03	150
Paper and cardboard	0.87	0.84	0.89	0.01	180
Mixed CDWs	0.87	0.84	0.93	0.02	5280 [1]

[1] Number of ROIs considered.

It is worthy to note that for the mixed CDWs class the emissivity values were calculated considering the ROIs of all the frames from all the tests, the sum of which gives the number of measurements in Table 3. Figure 7 shows the distribution of the emissivity values of mixed CDWs class. The number of occurrences is the total number of ROIs.

An alternative representation of the results is provided in Figure 8, where bar graphs depict the mean and standard deviation for each class, using a coverage factor $k = 2$ in order to have 95 % confidence intervals.

The results indicate that certain classes have a tight emissivity interval, which suggests low inter-specimen variability within the class; examples of such materials include tiles and ceramics (on both sides), and paper and cardboard. In contrast, other classes, such as plastics, metals and wood, show higher inter-specimen variability; this is due to the heterogeneity of specimens within these classes, especially in the plastic category, which includes different types of plastic materials.

3.2. Results of the uncertainty analysis

The results of the uncertainty analysis, performed on four classes, are shown in Table 4. The input uncertainty ($u(x_i)$) represents the uncertainty associated with the emissivity value of the reference paint (x_i), while the output uncertainty ($u_i(y)$) corresponds to the obtained uncertainty in the emissivity value of the material to be characterized (y) for that specific test. The mean values obtained from the Monte Carlo simulation are very similar to (or equal to) the respective mean values displayed in Table 3, and therefore are not shown.

Table 4. Results of MCM-based uncertainty analysis on IR thermography results related to the different test performed: 1) single test on a single specimen, 2) 3 repeated tests on a same specimen, and 3) 3 repeated tests on 5 different specimens. Input ($u(x_i)$) and output ($u_i(y)$) uncertainty for each material and test.

Material	Test 1		Test 2		Test 3	
	$u(x_i)$	$u_i(y)$	$u(x_i)$	$u_i(y)$	$u(x_i)$	$u_i(y)$
Concrete	0.01	0.02	0.01	0.02	0.01	0.02
Brick	0.01	0.02	0.01	0.02	0.01	0.02
Plastic	0.01	0.02	0.01	0.03	0.01	0.04
Paper and cardboard	0.01	0.02	0.01	0.02	0.01	0.02

For the classes concrete, brick, and paper and cardboard, the values of the mean and standard deviation are very similar (or equal) between the three tests. This indicates that specimens are very similar to each other and both intra- and inter-specimen variability are limited and acceptable. On the other hand, the values change for plastic; in particular, the standard deviation increases from the first to the third test and this is due to the heterogeneity of the specimens of this material (i.e., high inter-specimen variability) compared to the specimens of the other classes, which are more similar to each other, hence providing a better repeatability.

Examples of the distribution of reference and test materials emissivity values are reported in Figure 9 and Figure 10. In Figure 9 the class is concrete, and the test is the first one (i.e., single test on a single specimen); the output uncertainty is approximately doubled with respect to the input one, with an expanded uncertainty ($k = 2$) of 0.04. In Figure 10 the class is plastic, and the test is the third one (i.e., 3 repeated tests on 5 different specimens), where the output uncertainty is the highest of all the tests (0.04), including also the contribution of repeated tests and specimens variability. These two cases were chosen to be represented because they are the ones with the lowest and highest output uncertainty.

Active thermography for estimating material emissivity has proven to be a valid technique; however, observing the results it is clear that it is not possible to univocally distinguish the type of material based solely on this estimation. In fact, the emissivity ranges of the materials of interest often overlap, and for some materials, such as plastics and metals, the ranges (from minimum- to maximum) are very wide; this is due to the intrinsic variability of the different types of plastics and metals among themselves. As a result, the measurements are compatible, and the classes are not distinguishable from each other.

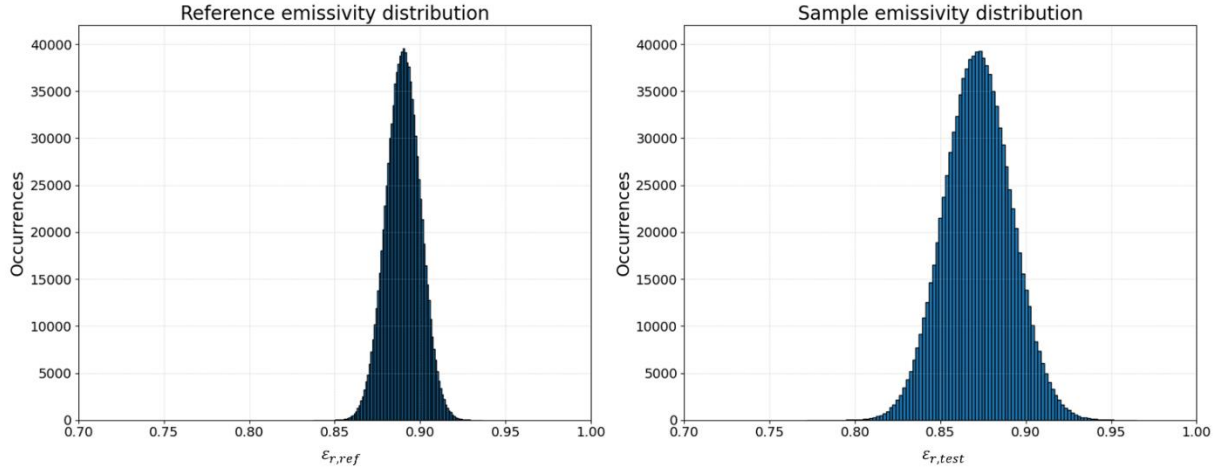

Figure 9. Probability distribution of reference (left, input) and test (right, output) emissivity values; test n. 1 on concrete class (dataset related to a single test performed on a single specimen).

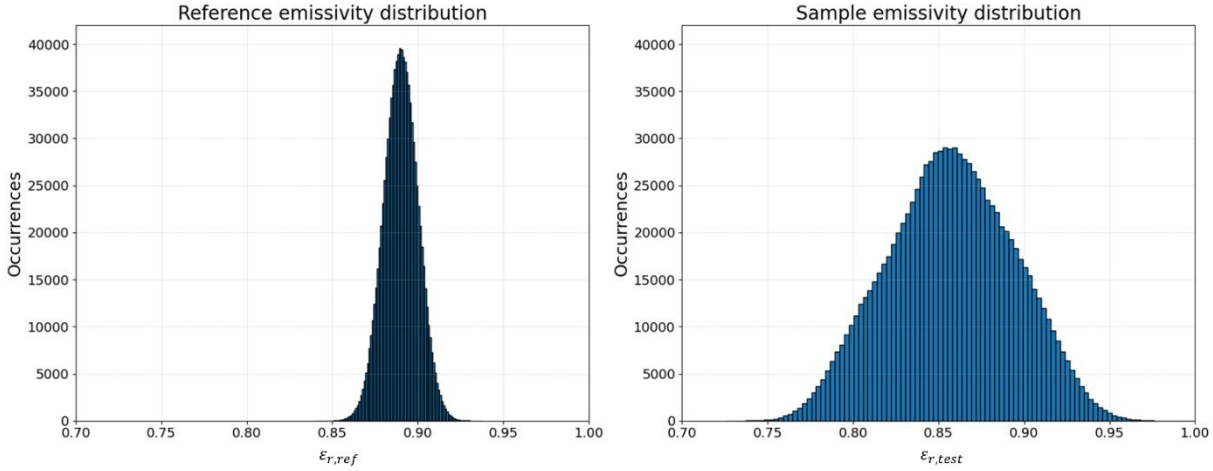

Figure 10. Probability distribution of reference (left, input) and test (right, output) emissivity values; test n. 3 on plastic class (dataset related to repeated tests on different specimens).

4. CONCLUSIONS

In this study active thermography, supported by a statistical assessment, was evaluated as a potential source of information for the classification technique for several CDWs material classes based on the emissivity values, particularly the hemispherical spectral emissivity. Multiple tests were conducted on different specimens collected from waste management or construction sites, and the overall results were expressed as confidence intervals in order to properly consider the materials variability. Moreover, a measurement uncertainty analysis based on the Monte Carlo method was performed to express the measurement uncertainty as recommended by the GUM.

The CDWs classification based solely on these thermographic data is not feasible, but for sure the information is relevant also to perform precise non-contact temperature measurements (that could be useful in-field, for example, to check the proper temperature for material transportation by trucks). The measurement uncertainty analysis showed a limited variability for all the classes (expanded uncertainty of $\pm$ 0.04, with a coverage factor $k = 2$, with the exception of plastic class that reported a doubled uncertainty – presumably linked to the multiple sub-classes of plastic specimen analysed).

Due to the limitation of the amount of data used, the proposed approach can be considered as a preliminary study in this field; in particular, it is worthy to underline that more accurate and widely extendable results can be achieved analysing a larger number of specimens per class; also, it would be interesting to perform the tests considering sub-classes of certain materials (e.g., plastics and metals).

For sure, data-fusion from different sensors also operating in diverse spectral ranges can result beneficial since the final output provides a broader overview of the material to be characterised. Active thermography could be combined with other non-contact sensors, such as visible or hyperspectral cameras, and their use could enable different and complementary features to be extracted from materials. By leveraging information from different sensors, it would be possible to obtain a more complete characterization of CDWs materials, and an efficient classification method also based on ML and AI techniques.

This information can be exploited in a view of CDWs valorisation, going towards a more sustainable and circular construction sector according to the European Commission guidelines and recommendations [29].

AUTHORS' CONTRIBUTION

Giovanni Salerno: Conceptualization, Data curation, Software, Formal analysis, Investigation, Writing – original draft.

Gloria Cosoli: Conceptualization, Investigation, Supervision, Writing – review & editing.

Maria Teresa Calcagni: Conceptualization, Data curation, Software, Investigation, Writing – original draft.

Giuseppe Pandarese: Conceptualization, Investigation, Writing – review & editing.

Gian Marco Revel: Project administration, Supervision, Writing – review & editing.

ACKNOWLEDGEMENT

This research activity was carried out within the RECONSTRUCT (A Territorial Construction System for a Circular Low-Carbon Built Environment) project, funded by the European Union's Horizon Europe research and innovation programme under grant agreement no. 101082265.

REFERENCES

[1] 74 authors, Materials 2030 RoadMap, 2022. Online [Accessed 9 September 2024] https://prod5.assets-cdn.io/event/7788/assets/8344205751-b86a937e20.pdf

[2] E. Koroxenidis, A. Karanafti, K. Tsikaloudaki, T. Theodosiou, Towards the digitalization and automation of circular and sustainable construction and demolition waste management – project RECONMATIC, IOP Conf. Ser. Earth Environ. Sci., vol. 1196, no. 1, p. 012044, Jun. 2023. DOI: 10.1088/1755-1315/1196/1/012044

[3] P.-Y. Wu, C. Sandels, K. Mjörnell, M. Mangold, T. Johansson, Predicting the presence of hazardous materials in buildings using machine learning, Build. Environ., vol. 213, Apr. 2022, p. 108894. DOI: 10.1016/j.buildenv.2022.108894

[4] S. Dodampegama, L. Hou, E. Asadi, G. Zhang, S. Setunge, Revolutionizing construction and demolition waste sorting: Insights from artificial intelligence and robotic applications, Resour. Conserv. Recycl., vol. 202, Mar. 2024, p. 107375. DOI: 10.1016/j.resconrec.2023.107375

[5] I. Vegas, K. Broos, P. Nielsen, O. Lambertz, A. Lisbona, Upgrading the quality of mixed recycled aggregates from construction and demolition waste by using near-infrared sorting technology, Constr. Build. Mater., vol. 75, Jan. 2015, pp. 121-128. DOI: 10.1016/j.conbuildmat.2014.09.109

[6] S. Serranti, R. Palmieri, G. Bonifazi, Hyperspectral imaging applied to demolition waste recycling: innovative approach for product quality control, J. Electron. Imaging, vol. 24, no. 4, Jul. 2015, p. 043003. DOI: 10.1117/1.JEI.24.4.043003

[7] G. Bonifazi, G. Capobianco, S. Serranti, Hyperspectral Imaging and Hierarchical PLS-DA Applied to Asbestos Recognition in Construction and Demolition Waste, Appl. Sci., vol. 9, no. 21, Oct. 2019, p. 4587. DOI: 10.3390/app9214587

[8] S. Zhang, Y. Chen, Z. Yang, H. Gong, Computer Vision Based Two-stage Waste Recognition-Retrieval Algorithm for Waste Classification, Resour. Conserv. Recycl., vol. 169, June 2021, p. 105543. DOI: 10.1016/j.resconrec.2021.105543

[9] W. Lu, J. Chen, F. Xue, Using computer vision to recognize composition of construction waste mixtures: A semantic segmentation approach, Resour. Conserv. Recycl., vol. 178, Mar. 2022, p. 106022. DOI: 10.1016/j.resconrec.2021.106022

[10] G. Cosoli, G. Salerno, M. T. Calcagni, G. Pandarese, L. Violini, E. El Masri, H. De Melo Ribeiro, M. A. A. Abbas, G. M. Revel, How to Valorize Construction and Demolition Wastes? Beyond the State of the art Through Vision Systems and Artificial Intelligence Tools, Proc. of the IEEE Int. Workshop Metrol. Living Environ. MetroLivEnv 2024, Chania, Greece, 12-14 June 2024, pp. 552–557. DOI: 10.1109/ MetroLivEnv60384.2024.10615834

[11] F. K. Konstantinidis, S. Sifnaios, G. Tsimiklis, S. G. Mouroutsos, A. Amditis, A. Gasteratos, Multi-sensor cyber-physical sorting system (CPSS) based on Industry 4.0 principles: A multi-functional approach, Procedia Comput. Sci., vol. 217, 2023, pp. 227-237. DOI: 10.1016/j.procs.2022.12.218

[12] G. Bonifazi, O. Trotta, G. Capobianco, S. Serranti, Characterization of post-earthquake construction and demolition wastes by Hyperspectral imaging, 7th Int. Conf. Ind. Hazard. Waste Manag., 2021. Online [Accessed 22 August 2024] https://iris.uniroma1.it/handle/11573/1603025

[13] M. Nyumura, Y. Bao, Selection of construction waste using sensor fusion, Electron. Imaging, vol. 31, no. 7, Jan. 2019, pp. 456-1–456–6.
DOI: 10.2352/ISSN.2470-1173.2019.7.IRIACV-456

[14] F. Radica, G. Iezzi, O. Trotta, G. Bonifazi, S. Serranti, J. De Brito, Characterization of CDW types by NIR spectroscopy: Towards an automatic selection of recycled aggregates, J. Build. Eng., vol. 88, Jul. 2024, p. 109005.
DOI: 10.1016/j.jobe.2024.109005

[15] A. Mobili, M. T. Calcagni, G. M. Revel, (+ another 7 authors), How to Quickly Characterize Construction and Demolition Wastes? Traditional and Advanced Portable Solutions in Comparison, Proc. of the IEEE Int. Workshop on Metrology for Living Environment (MetroLivEnv), Chania, Greece, 12-14 June 2024, pp. 558–563.
DOI: 10.1109/MetroLivEnv60384.2024.10615486

[16] S. P. Gundupalli, S. Hait, A. Thakur, Classification of metallic and non-metallic fractions of e-waste using thermal imaging-based technique, Process Saf. Environ. Prot., vol. 118, Aug. 2018, pp. 32–39.
DOI: 10.1016/j.psep.2018.06.022

[17] S. P. Gundupalli, S. Hait, A. Thakur, Multi-material classification of dry recyclables from municipal solid waste based on thermal imaging, Waste Manag., vol. 70, Dec. 2017, pp. 13–21.
DOI: 10.1016/j.wasman.2017.09.019

[18] H. Bai, T. Bhattacharjee, H. Chen, A. Kapusta, C. C. Kemp, Towards Material Classification of Scenes Using Active Thermography, Proc. of the IEEE/RSJ Int. Conf. on Intelligent Robots and Systems (IROS), Madrid, Spain, 1-5 October 2018, pp. 4262–4269.
DOI: 10.1109/IROS.2018.8594469

[19] S. Mineo, G. Pappalardo, Rock Emissivity Measurement for Infrared Thermography Engineering Geological Applications, Appl. Sci., vol. 11, no. 9, Apr. 2021, p. 3773.
DOI: 10.3390/app11093773

[20] M. J. M. Harrap, S. A. Rands, Floral infrared emissivity estimates using simple tools, Plant Methods, vol. 17, no. 1, Dec. 2021, p. 23.
DOI: 10.1186/s13007-021-00721-w

[21] Y. Lv, J. Wu, W. Yang, Y. Xiang, H. Wang, X. Zhu, Q. Liao, Approaching the emissivity of CMAS at high temperatures by convenient thermocouple-based infrared thermography, Int. J. Heat Mass Transf., vol. 232, p. 125975, Nov. 2024.
DOI: 10.1016/j.ijheatmasstransfer.2024.125975

[22] Commission of the European communities, EUROSTAT, Guidance on classification of waste according to EWC-Stat categories, 2010. Online [Accessed 17 March 2023]
https://circabc.europa.eu/ui/group/b01d2930-990e-44fb-9121-a9a6b00a1283/library/0ff9b070-ecd3-48b7-8e1f-e5d14c0f006a/details

[23] COMSA Corporación Infrastructure development and industrial engineering, Sobre COMSA Corporación. Online [Accessed 17 March 2024]
https://www.comsa.com/en/

[24] Sorigué business group, Sorigué website. Online [Accessed 17 March 2024]
https://www.sorigue.com/en

[25] X. P. V. Maldague, Theory and Practice of Infrared Technology for Nondestructive Testing. John Wiley & Sons, 2001.

[26] Infratec GmbH, Camera series VarioCAM® HD head security 900. Online [Accessed 17 March 2024]
https://www.infratec.eu/thermography/infrared-camera/variocam-hd-head-security-900/

[27] Aremco, High Temperature High Emissivity Coatings - Aremco HiE-Coat. Online [Accessed 17 March 2024]
https://www.aremco.com/high-emissivity-coatings/

[28] BIPM JCGM, Evaluation of measurement data-Guide to the expression of uncertainty in measurement - Évaluation des données de mesure-Guide pour l'expression de l'incertitude de mesure', 2008.

[29] G. M. Revel, E. M. Rodriguez Sierra, C. Partsch, Task force, White Paper on Sustainable Material-based Solutions For Energy Efficient Buildings, 2023. Online [Accessed 16 June 2025]
https://www.iwg5-buildings.eu/wp-content/uploads/2023/09/IWG5_New-materials_WP_31072023.Finalversion.pdf